# INVERTING AMPLITUDE VERSUS RAY PARAMETER CURVES USING THE REFLECTION IMPEDANCE CONCEPT

*L.T. Santos and M. Tygel*

**email:** *lucio@ime.unicamp.br*

**keywords:** *Reflection Impedance, Inversion, AVO, AVA, AVP*

**ABSTRACT**

*Amplitude versus offset (AVO) or amplitude versus angle (AVA) curves are nowadays regularly extracted from seismic data for various purposes of reservoir studies and characterization. Besides the information that can be obtained merely from their shape, AVO/AVA curves can also be used to invert more quantitative attributes, such as the intercept and the gradient of the reflection coefficient or, even better, the elastic-parameter contrasts. For a common-midpoint gather, the AVA curve is generally derived from its AVO counterpart by means of a well-known expression that relates the reflection angle to offset. The recently introduced reflection impedance concept provides an attractive approximation of the elastic PP-reflection coefficient as a function of the ray parameter. In this sense, that approximation can be of value when amplitude versus ray parameter (AVP) curves are available from seismic data. In this paper, we propose an algorithm to invert elastic-parameter contrasts from AVP curves using the reflection impedance approximation of the PP-reflection coefficient. First results shown on synthetic data indicate that the procedure may offer a promising alternative to existing methods of inverting reservoir attributes from AVO/AVA curves.*

## INTRODUCTION

The common midpoint (CMP) method, originally called the common depth point (CDP) method (see, e.g., Dix (1955)) is a classical procedure to produce both a simulated zero-offset (stacked) section and a corresponding time-domain velocity model defined throughout that section.

The procedure optimally stacks sorted out in CMP gathers, namely source-receiver pairs that are symmetrically located around a fixed point, the CMP. In the 2D situation of a single (horizontal) seismic line and within a given CMP gather, the stacking is carried out along the traveltime function

$$T(h) = \sqrt{T_0^2 + C\ h^2}\ , \tag{1}$$

called *Normal Moveout (NMO)*. In the above equation, $T(h)$ is the traveltime from the source to the reflector and back to the receiver, $h$ being the source-receiver half offset. At selected zero-offset (ZO) time samples, $T_0$, the parameter $C$ is determined as the one that maximizes the coherency (semblance) of the data along the traveltime (1). In this situation, $T_0$ is interpreted as the CMP ZO traveltime at the CMP and

$$C = \frac{4}{V_{NMO}^2}\ , \tag{2}$$

where $V_{NMO}$ is the NMO-velocity. The procedure, referred to as velocity analysis in the seismic literature, is carried out for all CMP locations and well-selected ZO time samples. After interpolation, an NMO-velocity field is determined at all CMP and ZO time samples. Finally, the ZO (stacked) output at each CMP and ZO time sample, $(X_m, T_0)$, is obtained by stacking the CMP gather defined by $X_m$ along the

NMO curve (1) using the given ZO time sample $T_0$ and the $C$ parameter defined by the NMO velocity $v_{NMO} = v_{NMO}(X_m, T_0)$.

Under the usual assumption of a horizontally stratified (or small-dip) media, the ray parameter for the reflection ray in the CMP gather can be approximated by (see, e.g., Castagna and Backus (1993)),

$$p = \frac{1}{2}\frac{d}{dh}T(h) = \frac{C}{2\sqrt{C + T_0^2/h^2}} \,. \tag{3}$$

From the well-known relationship

$$p = \frac{\sin\theta}{v}, \tag{4}$$

where $\theta$ is the incident angle at the reflector and $v$ is the interval velocity, the corresponding expression for the angle is

$$\sin\theta = \frac{Cv}{2\sqrt{C + T_0^2/h^2}} \,. \tag{5}$$

Note that, in the present situation of P-P reflections, the incident angle, $\theta$, at the reflector coincides with the corresponding reflection angle.

We recall that interval-velocity field, $v$, (in depth) has to be inverted from its corresponding NMO velocity field, $v_{NMO}$, by the well-known Dix algorithm (see, e.g., Hubral and Krey (1980)). In this way, ray parameters, as directly extracted from the seismic data, tend to be more reliable that their counterpart incident angles, that need an additional inversion to be obtained.

The following step is to perform an inversion based on the amplitudes versus ray parameter (AVP) of the CMP rays. Figure 1 ilustrates the described process for a synthetic model.

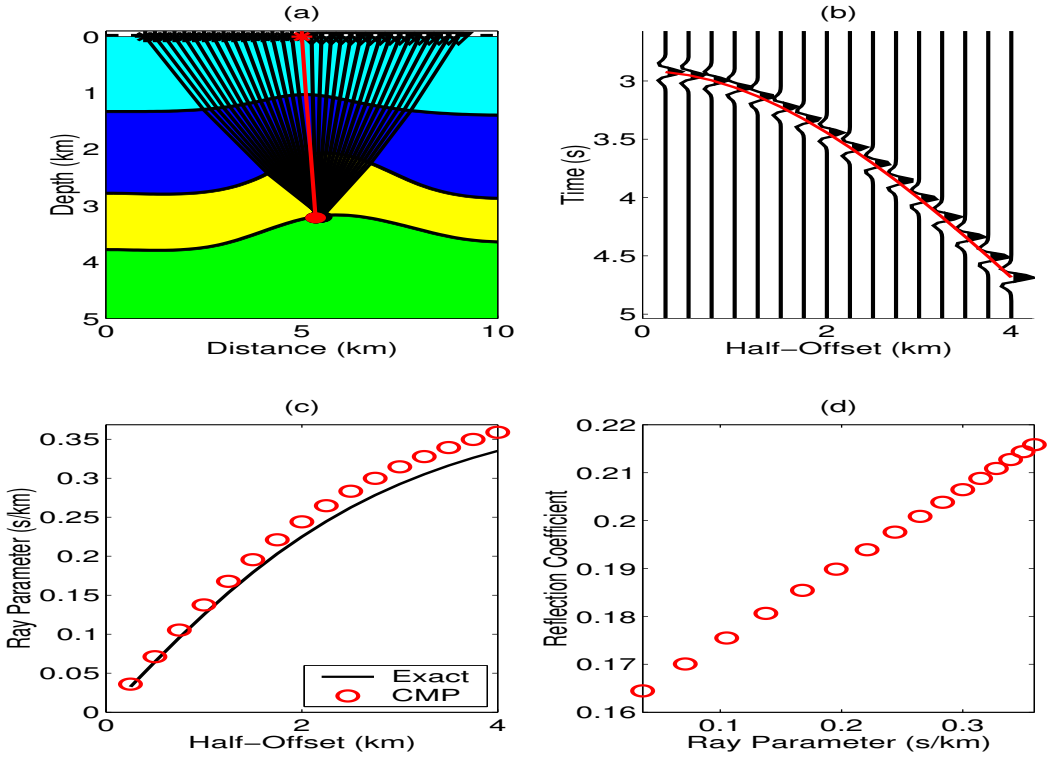


**Figure 1:** Example of an AVP analysis: (a) Synthetic model with CMP rays; (b) CMP section with fitted hyperbola; (c) Exact and extracted ray parameter; (d) Amplitude variation with ray parameter.

## VELOCITY ANALYSIS BY THE CRS METHOD

The common reflection surface (CRS) method, introduced by Peter Hubral and co-workers (see, e.g., Hubral et al. (1998)) represents a natural extension of the CMP method in two important aspects. Firstly, for each stacking trace location (now called simply a central point), the CRS considers a supergather of source-receiver pairs, arbitrarily located with respect to the central point. In other words, the gather is not restricted to the CMP condition. Secondly, not only the NMO velocity, but also other additional parameters are extracted from the data. In the present 2D situation, three parameters are determined for each central point and all ZO traveltime samplea. The procedure is performed automatically, with no *a priori* selection of traveltime samples.

To be able to stack source-receiver pairs that do not conform to the CMP condition, the CRS method utilizes the (generalized) hyperbolic moveout

$$T(x,h) = \sqrt{(T_0 + A\ x)^2 + B\ x^2 + C\ h^2}\ , \tag{6}$$

where $x$ and $h$ denote the midpoint (relative to the central point) and half-offset coordinates of the source and receiver pair, and $T_0$ is the ZO traveltime at the central point. As shown in Hubral et al. (1998), the parameters $A$, $B$ and $C$ are related to physical quantities referred to as the CRS parameters or attributes,

$$A = \frac{2\sin\phi}{v_0},\ B = \frac{2T_0\cos^2\phi}{v_0}K_N,\ C = \frac{2T_0\cos^2\phi}{v_0}K_{NIP}, \tag{7}$$

where $\phi$ is the emergence angle of the ZO ray with respect to the surface normal, and $K_N$ and $K_{NIP}$ are the curvatures of the N- and NIP-waves, respectively (see Hubral (1983)). All these quantities are evaluated at the central point. Finally, $v_0$ denotes the medium velocity, also at the central point. Observe that formula (6) reduces to the normal-moveout (1) in the case of a CMP gather, i.e., $x = 0$. Moreover, the relation between $V_{NMO}$ and the CRS parameters is clear,

$$V_{NMO}^2 = \frac{4}{C} = \frac{2\ v_0}{T_0\ \cos^2\phi\ K_{NIP}}\ . \tag{8}$$

As described in Hubral (1983), the NIP-wave is a fictitious wave that starts at the reflection point of the ZO ray. This point is called normal-incident-point or NIP and progresses upwards with half the velocity of the medium. The N-wave is also a fictitious wave that starts as a wavefront that coincides with the reflector in the vicinity of the NIP. It is instructive to emphasize that the NIP-wave concept (with no special name), as well as the relation (8) between its curvature and the NMO velocity has been previously described in Chernyak and Gritsenko (1979).

The CRS method can be also used to perform an amplitude versus ray-parameter analysis, in the same way as it is done in the CMP method. The advantage of the CRS strategy is that the semblance analysis is applied for a grid of possible values for the central point and ZO traveltimes, using all gathers and not only the CMP ones. It is expected that the greater redundancy used by the CRS method, together with some average and smoothing procedures, should provide a more reliable NMO velocity field. A confirmation of this has been recently reported in Perroud and Tygel (2005).

The CRS method provides, as part of its output, a coherence section, in which the semblance value is assigned to each point at the stacked section. By examining the coherence section, it is possible to select regions with high values of the semblance function and then focus the attention at these regions. In Figure 2, we show the semblance panel obtained from the CRS method applied to the same synthetic model in Figure 1(a), together with the respective $C$-parameter panel.

## REFLECTION IMPEDANCE

As introduced in Connolly (1999) and discussed in Santos and Tygel (2004), it is possible to define an impedance function ($I$), for which the P-P reflection coefficient can be approximated in the appealing form

$$R_{PP} = \frac{I(\rho_2,\alpha_2,\beta_2,p) - I(\rho_1,\alpha_1,\beta_1,p)}{I(\rho_2,\alpha_2,\beta_2,p) + I(\rho_1,\alpha_1,\beta_1,p)}\ . \tag{9}$$

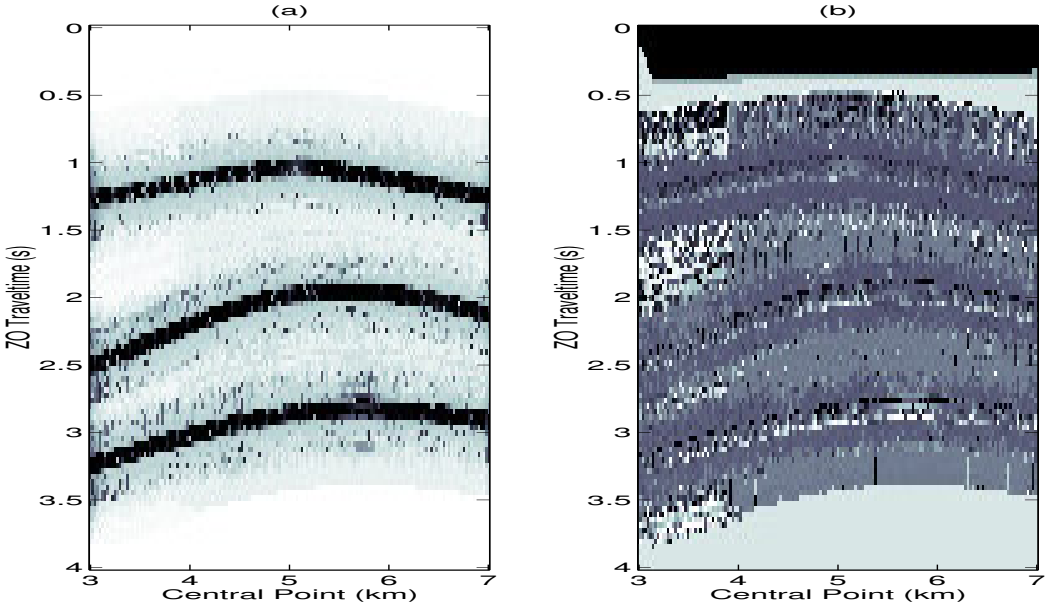


**Figure 2:** (a) Semblance panel obtained from the CRS method applied to the same synthetic model in Figure 1(a); (b) $C$-parameter panel.

In the above expression, $\rho_j$, $\alpha_j$, $\beta_j$ denote the density and P- and S-wave velocities at the incident side $(j = 1)$ and at the opposite side $(j = 2)$ of the reflecting interface, respectively. Moreover, $p$ is the ray parameter given by $p = \sin\theta/\alpha_1$ and $\theta$ is the incidence angle.

In its general form, equation (9), does not allow for a closed-form impedance function $I$ that adequately approximates the P-P reflection coefficient for arbitrary elastic parameters $\rho$, $\alpha$, and all ray parameters $p$. Therefore, some additional constraints are required. Santos and Tygel (2004) consider a Gardner's type relationship between $\rho$ and $\beta$,

$$\rho = b\,\beta^{\gamma}\ , \tag{10}$$

where $b$ and $\gamma$ are constants. Such constraint leads to the reflection impedance function

$$I = \frac{\rho\,\alpha}{\sqrt{1-\alpha^2 p^2}}\ \exp\{-2[2+\gamma]\beta^2 p^2\}\ . \tag{11}$$

Replacing the condition (10) by

$$K = \beta^2/\alpha^2, \tag{12}$$

where $K$ is a constant, the elastic impedance function,

$$I = \rho^{1\,-\,4K\sin^2\theta}\ \alpha^{\sec^2\theta}\ \beta^{-8K\sin^2\theta}\ . \tag{13}$$

earlier introduced in Connolly (1999) and formulated using the incident angle, $\theta$, instead of ray parameter $p$ is obtained.

In practical situations, both the reflection impedance constants, $b$ and $\gamma$, as well as the elastic impedance constant, $K$ are to be estimated using well-log information in the area.

In Figure 3 we compare the approximation formula (9), using (11) and (13), and the linear approximation of Aki and Richards (1980), for a representative elastic model. Observe the accuracy of the reflection impedance function, even for angles within the critical range.

## AVP INVERSION

The previous two sections have shown that (a) ray parameters can be well recovered from the seismic data and (b) the P-P reflection coefficient can be reliably approximated in terms of reflection impedances. From the above considerations, we now address the main topic of this paper, namely the inversion of AVP curves.

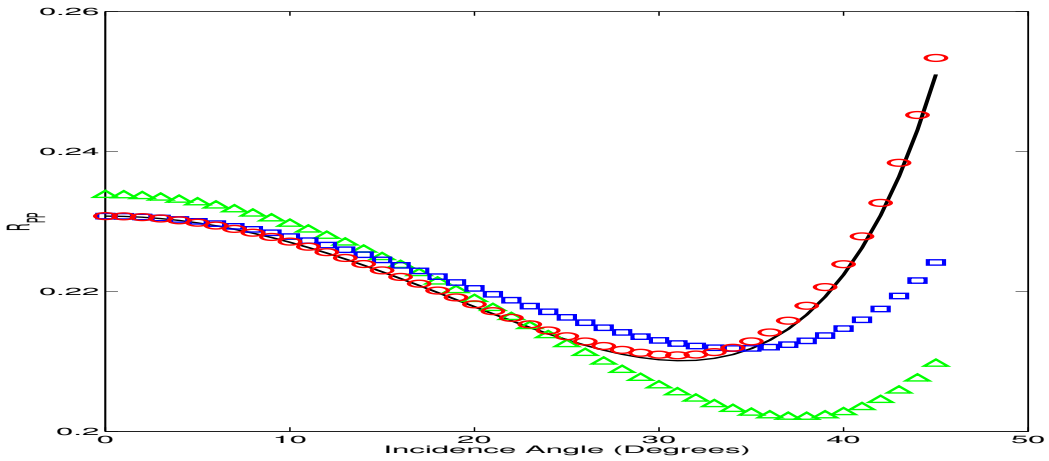


**Figure 3:** Approximations for $R_{PP}$: Exact (—), Linear ($\Delta$), Elastic Impedance ($\Box$), and Reflection Impedance ($\circ$).

Before starting the description of the inversion procedure, it is convenient to recast the reflection coefficient expression (9) in a form more suitable for the algorithm. From equations (9) and (11) we write

$$R_{PP}(p) = \frac{J(p) - 1}{J(p) + 1} \, , \tag{14}$$

where

$$J(p) = \frac{I(\rho_2, \alpha_2, \beta_2, p)}{I(\rho_1, \alpha_1, \beta_1, p)} = \frac{\rho_2 \, \alpha_2}{\rho_1 \, \alpha_1} \sqrt{\frac{1 - \alpha_1^2 \, p^2}{1 - \alpha_2^2 \, p^2}} \, \exp\{-2[2 + \gamma](\beta_2^2 - \beta_1^2)\} \, . \tag{15}$$

For the inversion, we now write

$$J(p) = \Lambda_3 \sqrt{\frac{1 - \Lambda_1^2 \, p^2}{1 - \Lambda_2^2 \, p^2}} \, \exp\{\Lambda_4 \, p^2\} \, , \tag{16}$$

where

$$\Lambda_1 = \alpha_1, \quad \Lambda_2 = \alpha_2, \quad \Lambda_3 = \frac{\rho_2 \, \alpha_2}{\rho_1 \, \alpha_1}, \quad \text{and } \Lambda_4 = -2[2 + \gamma](\beta_2^2 - \beta_1^2) \, . \tag{17}$$

Given a set of ray-parameters $\{p_n\}$ and the respectives reflection coefficients,$\{R_n\}$, we can apply a least-squares procedure to invert for the parameters $\Lambda_i$. The optimization problem to be solved is then

$$\min_{\Lambda_i} \sum_{n=1}^{N} \left[ R_n - \frac{J(p_n) - 1}{J(p_n) + 1} \right]^2 \, . \tag{18}$$

After the optimal solution is found, we compute the inverted ratios for P-wave velocity and density,

$$\frac{\alpha_2}{\alpha_1} = \frac{\Lambda_2}{\Lambda_1}, \quad \text{and} \quad \frac{\rho_2}{\rho_1} = \Lambda_3 \, \frac{\Lambda_1}{\Lambda_2} \, . \tag{19}$$

To extract the ratio for the S-wave velocity, additional information about the data is needed. For example, from a well-log analysis, if we estimate the value of the constant $\gamma$ in equation (10), then

$$\frac{\beta_2}{\beta_1} = \left( \frac{\rho_2}{\rho_1} \right)^{1/\gamma} \, . \tag{20}$$

## NUMERICAL EXPERIMENTS

A simple test on the accuracy of the AVP analysis presented above can be provided by the illustrative two-layer model depicted in Figure 4. For each interface, the values for the S-wave velocities, above and below the interface, are given by their corresponding P-wave velocity divided by $\sqrt{2}$ and $\sqrt{3}$, respectively. Densities are taken 1.2 g/cm$^3$ and 1.5 g/cm$^3$, above and below each interface, respectively. The CRS method, developed in Santos et al. (2005), was applied for central points $x_0$ and ZO traveltimes $T_0$ within the ranges $[3, 7]$ km and $[0, 4]$ s.

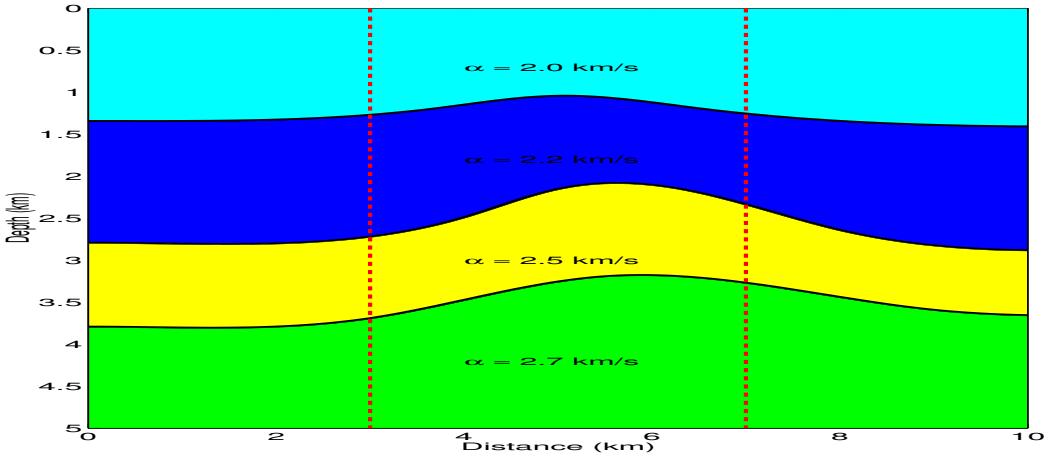


**Figure 4:** Synthetic model for the numerical experiments.

For each of the three interfaces, we select a box region with large values of the semblance function, and apply the inversion procedure for each $x_0$ in the box. We consider the two situations (a) using the correct values for the P-P reflection coefficient and (b) adding 10% noise. For the constant $\gamma$, from equation (20) we use the averaged value

$$\frac{1}{\gamma} = \frac{1}{3}\frac{\ln \sum_{j=1}^{3}[\beta_{j+1}/\beta_j]}{\ln(1.5/1.2)} = -0.4795\ . \tag{21}$$

Figures 5–7 show the results. Please observe that since the layers are homogeneous, each parameter ratio is constant along the $x_0$-axis for each reflector.

## CONCLUSIONS

We have addressed the problem of inversion of amplitude versus ray parameter (AVP) curves, using a combination of the CRS method and the formulation of the P-P reflection coefficient by means of the reflection impedance concept. The CRS method provides semblance and attribute panels, which yield information about the ray-parameter at the reflection point at target interfaces within the elastic model. The reflection impedance formulation, on the other hand, produces an approximation formula for the P-P reflection coefficient that is much suitable for inversion.

We have illustrated the inversion algorithm by applying it to a synthetic three-interface example, in which, for all interfaces, good approximations of all elastic-parameter contrasts were retrieved. The obtained numerical results indicate that the process has a good potential for real-data application.

## ACKNOWLEDGEMENTS

This work has been partially supported by CNPq (307165/2003-5 & 301733/2004-0) and FAPESP (01/01068-0), Brazil, and the sponsors of the Wave Inversion Technology (WIT) Consortium, Germany

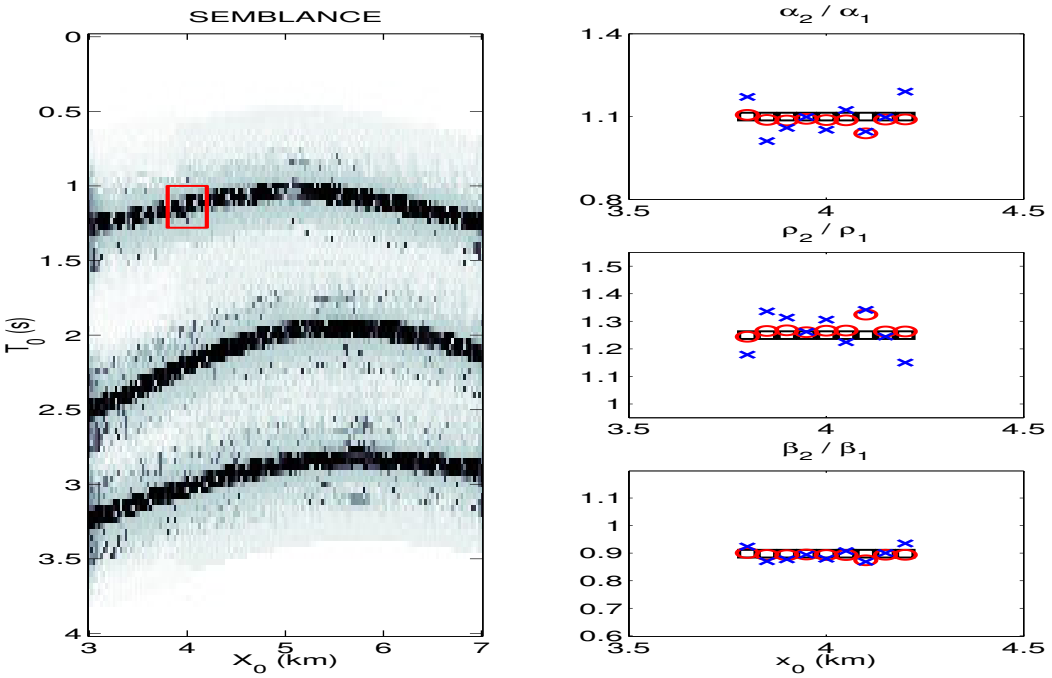


**Figure 5:** Parameter ratios for a window in the first reflector: Modelled (□), inverted without noise (○), and inverted with 10% noise (×).

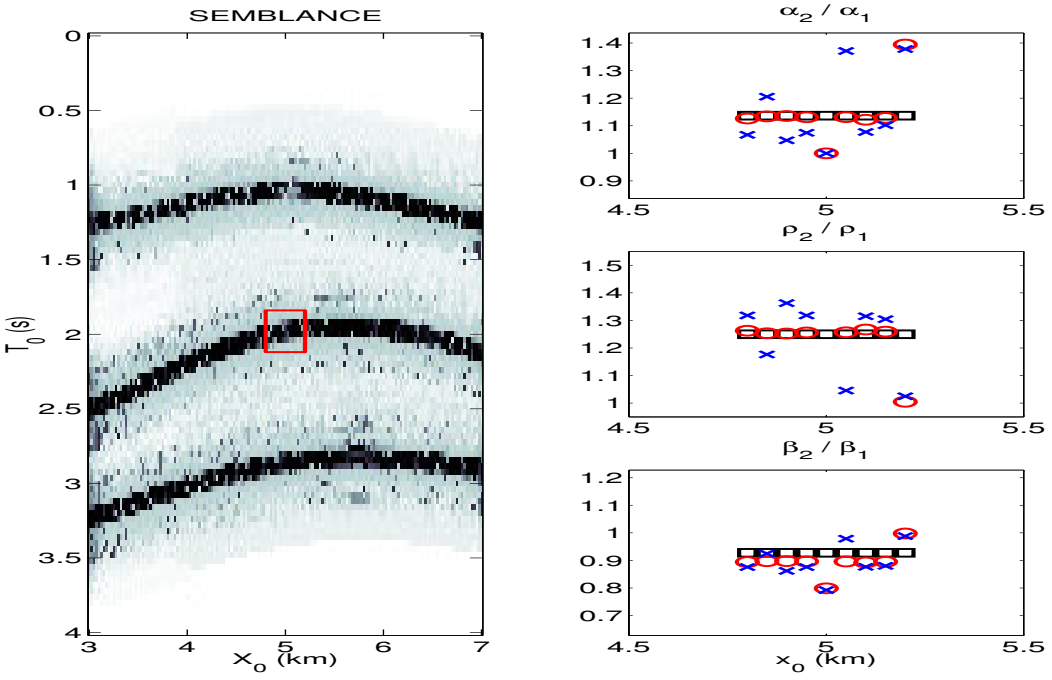


**Figure 6:** Parameter ratios for a window in the second reflector: Modelled (□), inverted without noise (○), and inverted with 10% noise (×).

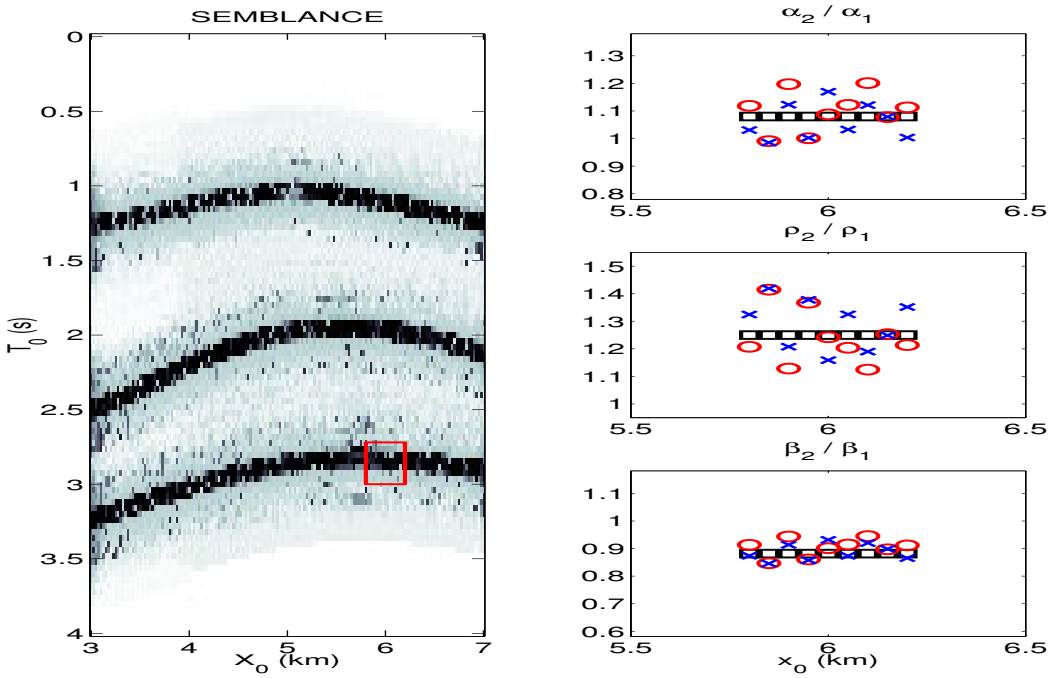


**Figure 7:** Parameter ratios for a window in the third reflector: Modelled (□), inverted without noise (○), and inverted with 10% noise (×).

## REFERENCES


Aki, K. and Richards, P. G. (1980). *Quantitative Seismology, Theory and Methods: Volume 1*. W. H. Freeman and Company.

Castagna, J. P. and Backus, M. M. (1993). *Offset-Dependent Reflectivity – Theory and Practice of AVO Analysis*. SEG.

Chernyak, V. S. and Gritsenko, S. A. (1979). Interpretation of the effective common-depth-point parameters for a three-dimensional system of homogeneous layers with curvilinear boundaries. *Geologiya i Geofizika*, 20:112–120.

Connolly, P. A. (1999). Elastic impedance. *The Leading Edge*, 18:438–452.

Dix, C. H. (1955). Seismic velocities from surface measurements. *Geophysics*, 20:68–86.

Hubral, P. (1983). Computing true amplitude reflections in a laterally inhomogeneous earth. *Geophysics*, 48:1051–1062.

Hubral, P., Höcht, G., and Jäger, R. (1998). An introduction to the common reflection surface stack. *60th EAGE Conference & Exhibition, Expanded Abstracts*, Session:01–19.

Hubral, P. and Krey, T. (1980). *Interval Velocities from Seismic Reflection Time Measurements*. SEG.

Perroud, H. and Tygel, M. (2005). Velocity estimation by the CRS method: Using GPR data. *Accepted by Geophysics*, 70.

Santos, L. T. and Tygel, M. (2004). Impedance-type approximations of the P-P elastic reflection coefficient: Modeling and AVO inversion. *Geophysics*, 69:592–598.

Santos, L. T., Yano, F., Salvatierra, M., Andreani, R., Martínez, J. M., and Tygel, M. (2005). A global optimization algorithm applied to the CRS problem. *Submitted to Journal of Seismic Exploration*.